

Supporting Information

SELF-ASSEMBLY OF N^3 -SUBSTITUTED XANTHINES IN THE SOLID STATE AND AT THE SOLID-LIQUID INTERFACE

Artur Ciesielski,^a Sébastien Haar,^a Attila Bényei,^b Gábor Paragi,^c Célia Fonseca Guerra,^d F. Matthias Bickelhaupt,^{d,e} Stefano Masiero,^f János Szolomájer,^g Paolo Samori,^{*,a} Gian Piero Spada,^{*,f} Lajos Kovács^{*,g}

^a Nanochemistry Laboratory, ISIS & icFRC, Université de Strasbourg & CNRS, 8 allée Gaspard Monge, 67000 Strasbourg, France.

^b University of Debrecen, Department of Physical Chemistry, Egyetem tér 1, 4010 Debrecen, Hungary.

^c Research Group of Supramolecular and Nanostructured Materials of the Hungarian Academy of Sciences, Dóm tér 8, 6720 Szeged, Hungary.

^d Department of Theoretical Chemistry and Amsterdam Center for Multiscale Modeling (ACMM), VU University Amsterdam, De Boelelaan 1083, NL-1081 HV Amsterdam, The Netherlands.

^e Radboud University Nijmegen, Institute for Molecules and Materials, Heyendaalseweg 135, NL-6525 AJ Nijmegen, The Netherlands.

^f Alma Mater Studiorum – Università di Bologna, Dipartimento di Chimica “G. Ciamician” Via San Giacomo 11 – 40126 Bologna, Italy.

^g University of Szeged, Department of Medicinal Chemistry, Dóm tér 8, 6720 Szeged, Hungary.

Table of Contents

1. NMR Spectroscopy and ESI study of N^3 -octadecylxanthine (compound 2)	S2
2. Polymeric structures based on N^9 -methylguanine	S6
3. X-ray powder patterns of N^3 -methylxanthine (compound 1)	S7
4. X-ray crystal structures of FADCUI and N^3 -methylxanthine (1)	S9
5. Theoretical studies	S13
Figure S1	S2
Figure S2	S3
Figure S3	S3
Figure S4	S4
Figure S5	S4
Figure S6	S5
Figure S7	S6
Figure S8	S7
Figure S9	S8
Figure S10	S11
Figure S11	S12
Table S1	S9
Table S2	S10
Table S3	S10
Table S4	S13

1. NMR Spectroscopy and ESI study of *N*³-octadecylxanthine (compound 2)

NMR spectra were recorded on a Varian Unity INOVA 600 MHz instrument equipped with a reverse probe. ESI-MS spectra were obtained with a Micromass ZMD-4000 spectrometer. Compound **2**, i.e. *N*³-octadecylxanthine was fully characterized by NMR. Signals were assigned on the basis of bidimensional spectra (Figs. S1-S5). Due to its low solubility, the compound was usually dissolved in high boiling solvents (DMSO or 1,1,2,2-tetrachloroethane) by heating, to improve *s/n* ratio.

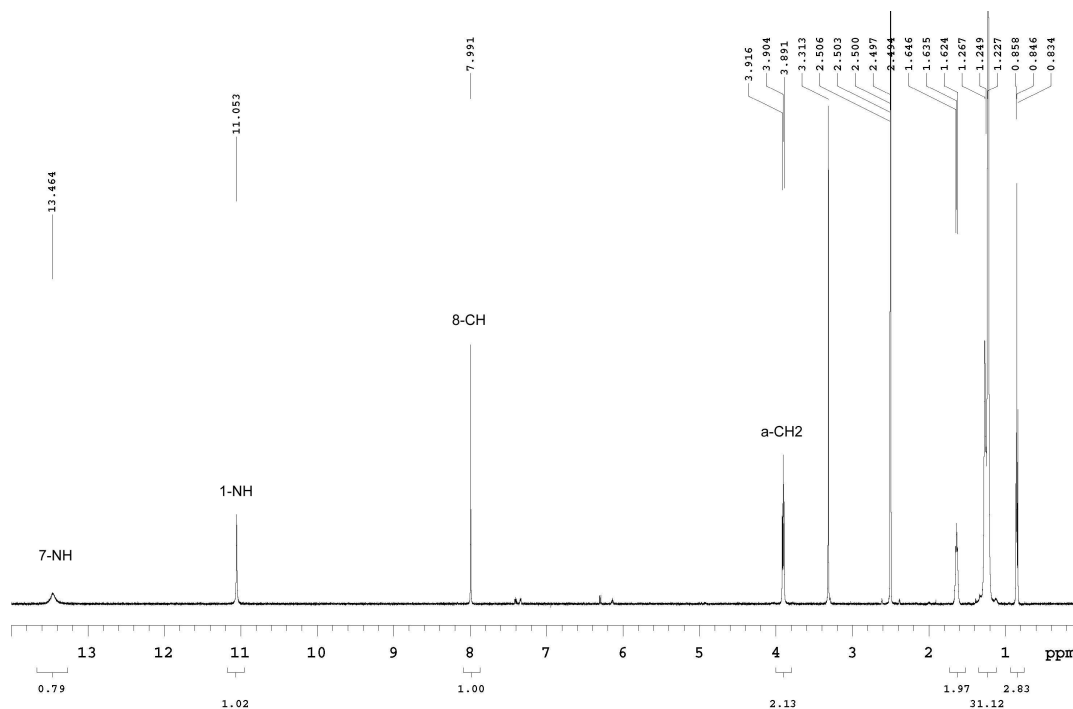


Figure S1. ¹H-NMR spectrum of compound **2** in DMSO-d₆ at r.t.

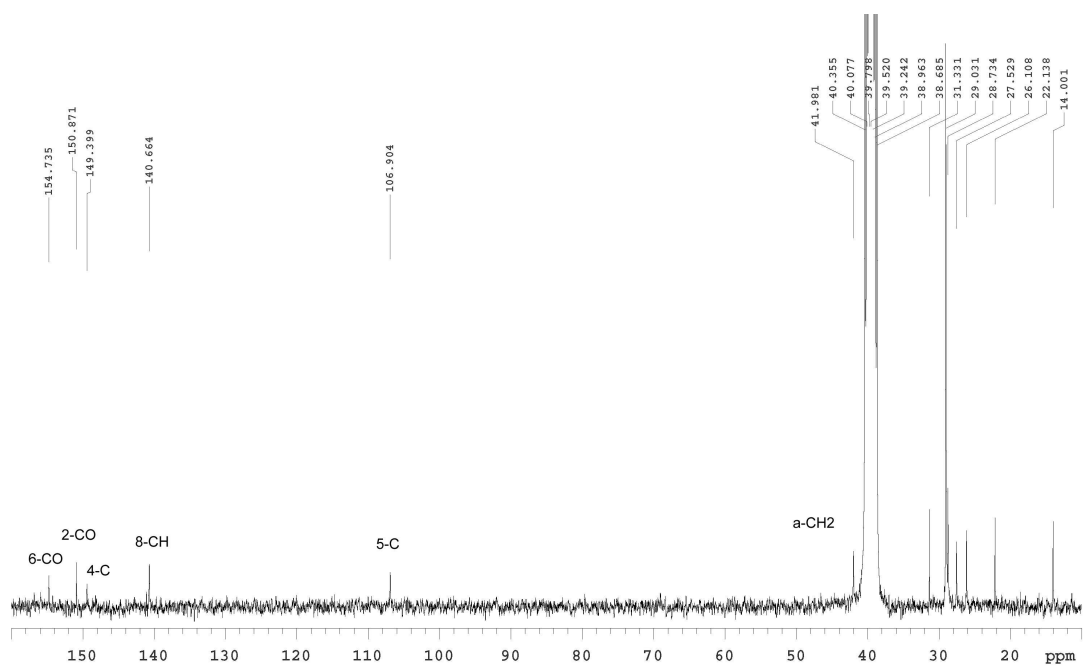


Figure S2. ¹³C NMR spectrum of compound **2** in DMSO-d₆ at r.t.

1600 std parameters
File:
Temp. 40.0 C / 313.1 K
Operator: sangiac
INOVA-600 "RHEL"

Relax. delay 1.000 sec
Acq. time 0.213 sec
Width 9611.9 Hz
2D Width 9611.9 Hz
4 repetitions
256 increments
OBSERVE H1, 599.7304205 MHz
DATA PROCESSING
Sine bell 0.107 sec
F1 DATA PROCESSING
Sine bell 0.027 sec
FT size 4096 x 4096
Total time 0 min 0 sec

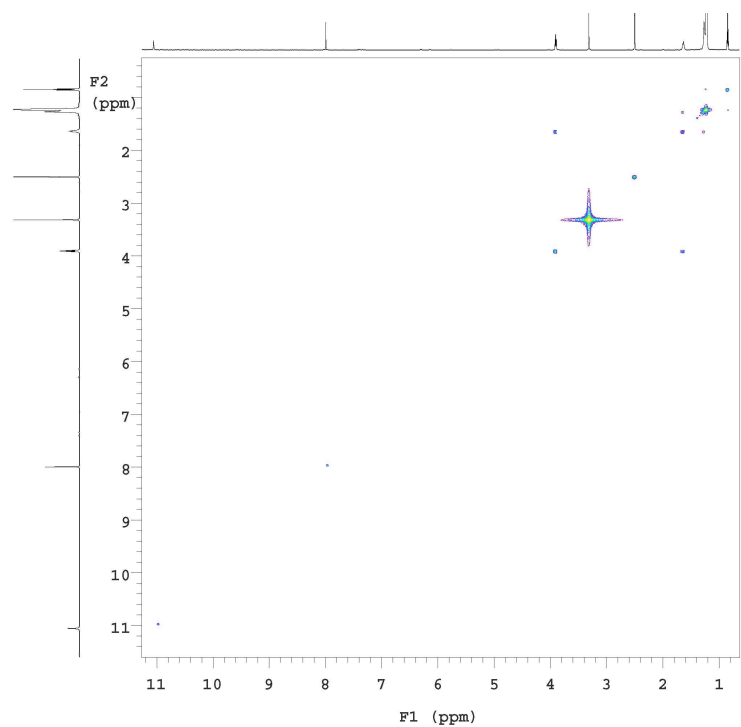


Figure S3. COSY spectrum of compound **2** in DMSO-d₆ at 40 °C

i600 std parameters

File:

Temp. 50.0 C / 323.1 K
Operator: sangiac
INOVA-600 "RHEL"

Relax. delay 1.000 sec
Mixing 0.500 sec
Acq. time 0.230 sec
Width 9611.9 Hz
2D Width 25632.8 Hz
64 repetitions

2 x 256 increments
OBSERVE H1, 599.7304197 MHz
DECOUPLE C13, 150.8136483 MHz
Power 43 dB
on during acquisition
off during delay
W40_Triple modulated
DATA PROCESSING
Gauss apodization 0.106 sec
F1 DATA PROCESSING
Gauss apodization 0.005 sec
FT size 8192 x 2048
Total time 0 min 0 sec

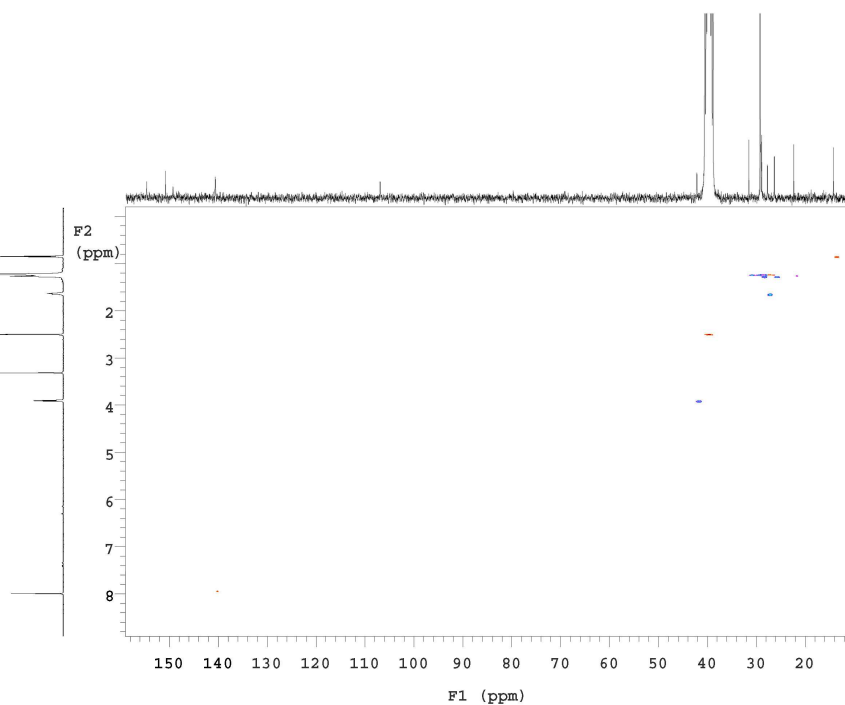


Figure S4. HSQC spectrum of compound **2** in DMSO- d_6 at 50 °C

i600 std parameters

File:

Temp. 40.0 C / 313.1 K
Operator: sangiac
INOVA-600 "RHEL"

Relax. delay 1.500 sec
Mixing 0.080 sec
Acq. time 0.128 sec
Width 9611.9 Hz
2D Width 36199.1 Hz
64 repetitions

256 increments
OBSERVE H1, 599.7304111 MHz
DATA PROCESSING
Sine bell 0.064 sec
F1 DATA PROCESSING
Sine bell 0.007 sec
FT size 4096 x 2048
Total time 0 min 0 sec

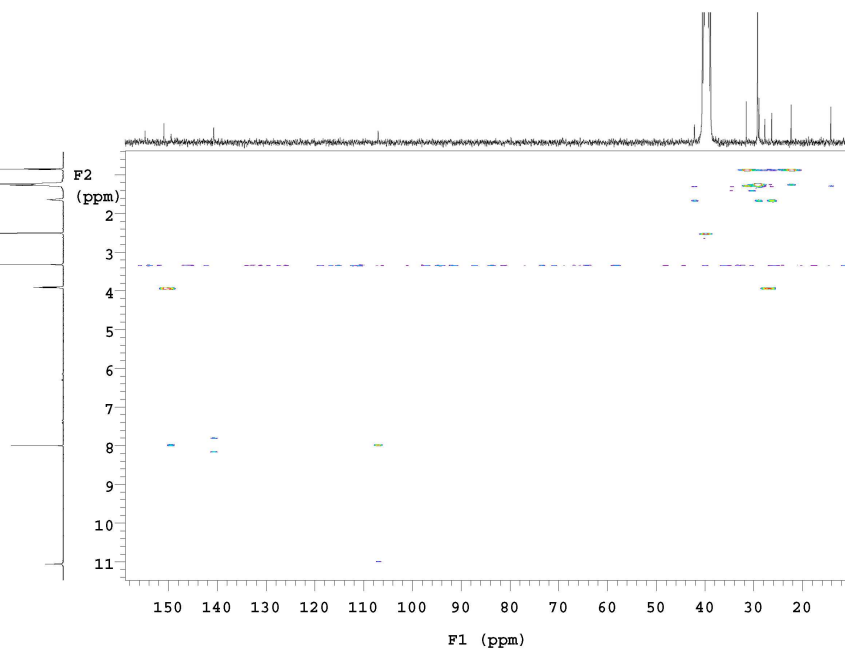


Figure S5. HMBC spectrum of compound **2** in DMSO- d_6 at 40 °C

Although no specific H-bonding pattern could be demonstrated by NMR investigations, some clues for the existence of H-bonded species (dimers or oligomers) in solution can be inferred. For instance, . 7-NH, 1-NH and H-8 peaks move upfield with temperature both in CD_2Cl_4 and in DMSO-d_6 (Fig. S6).

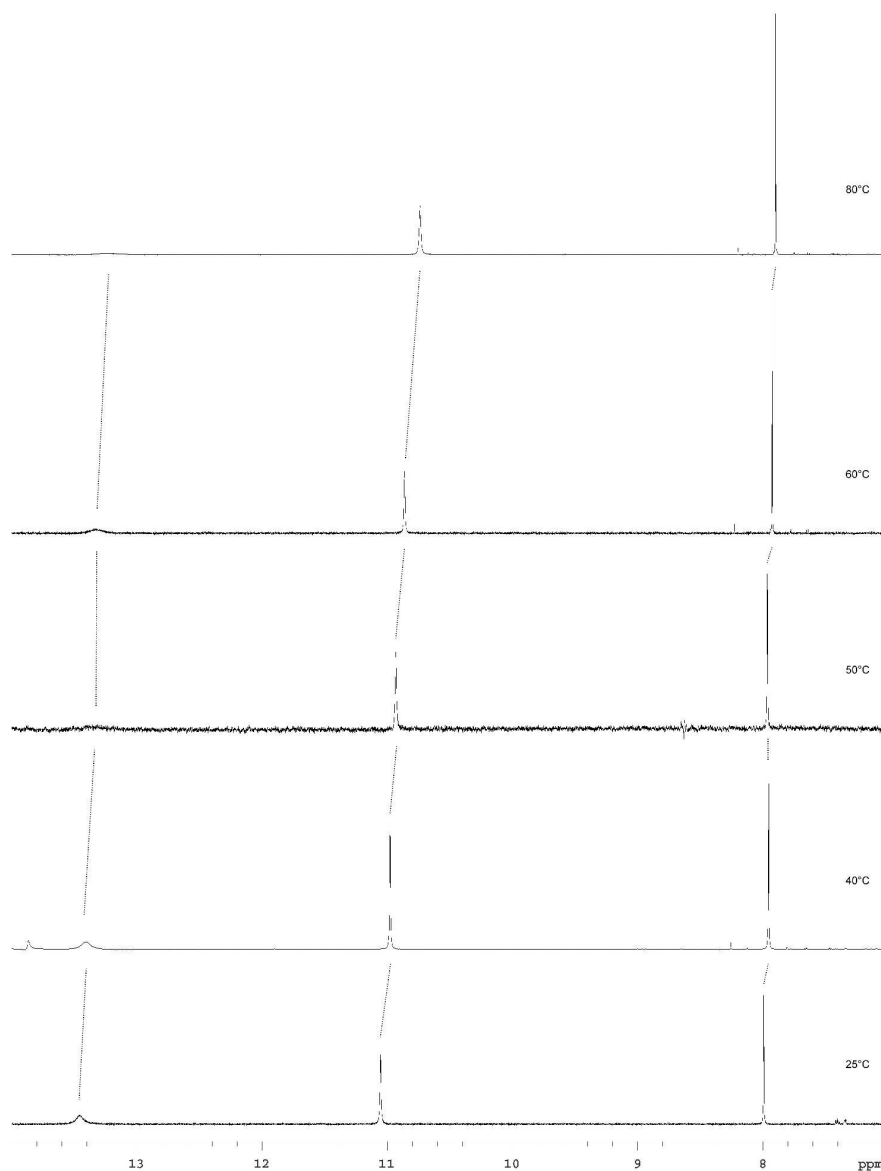


Figure S6. Downfield portion of ^1H -NMR spectra of compound **2** in DMSO-d_6 at different temperatures.

The ESI-MS (positive mode) spectrum of **2** in C₂H₂Cl₄/CHCl₃ solution shows as the main peaks signals corresponding to [(**2**)Na]⁺, [(**2**)₂Na]⁺, [(**2**)₃Na]⁺ and [(**2**)₄Na]⁺. The relative intensity of the last two peaks is indicative of the attitude of **2** to form ion-templated X-quartets (Fig. S7).

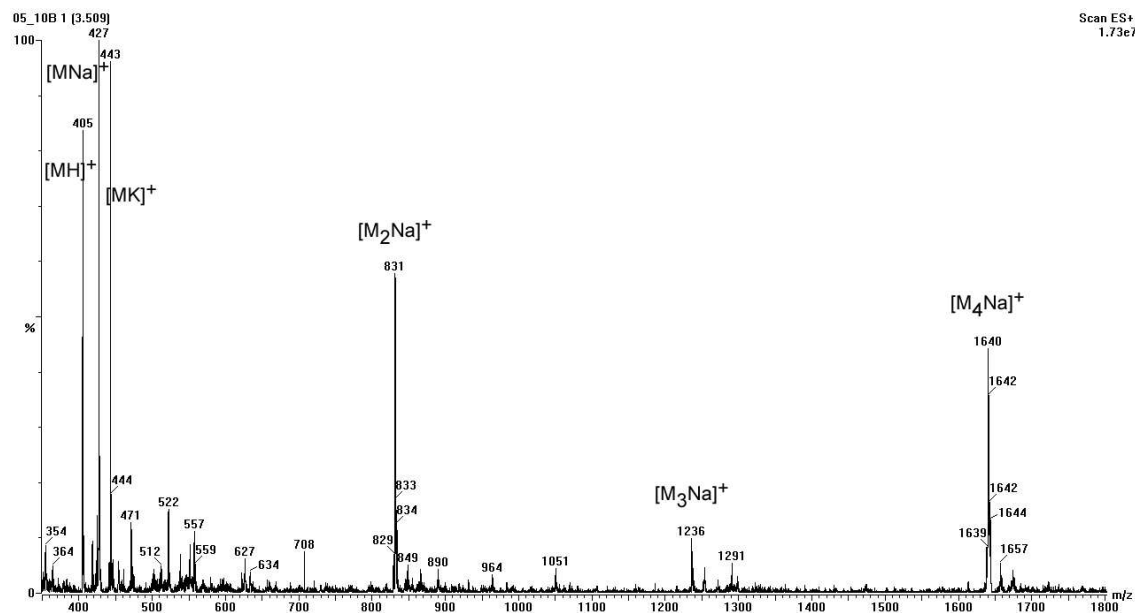


Figure S7. ESI-MS (positive mode) of compound **2** in C₂H₂Cl₄/CHCl₃ solution (with a small amount of formic acid added).

2. Polymeric structures based on N^9 -methylguanine

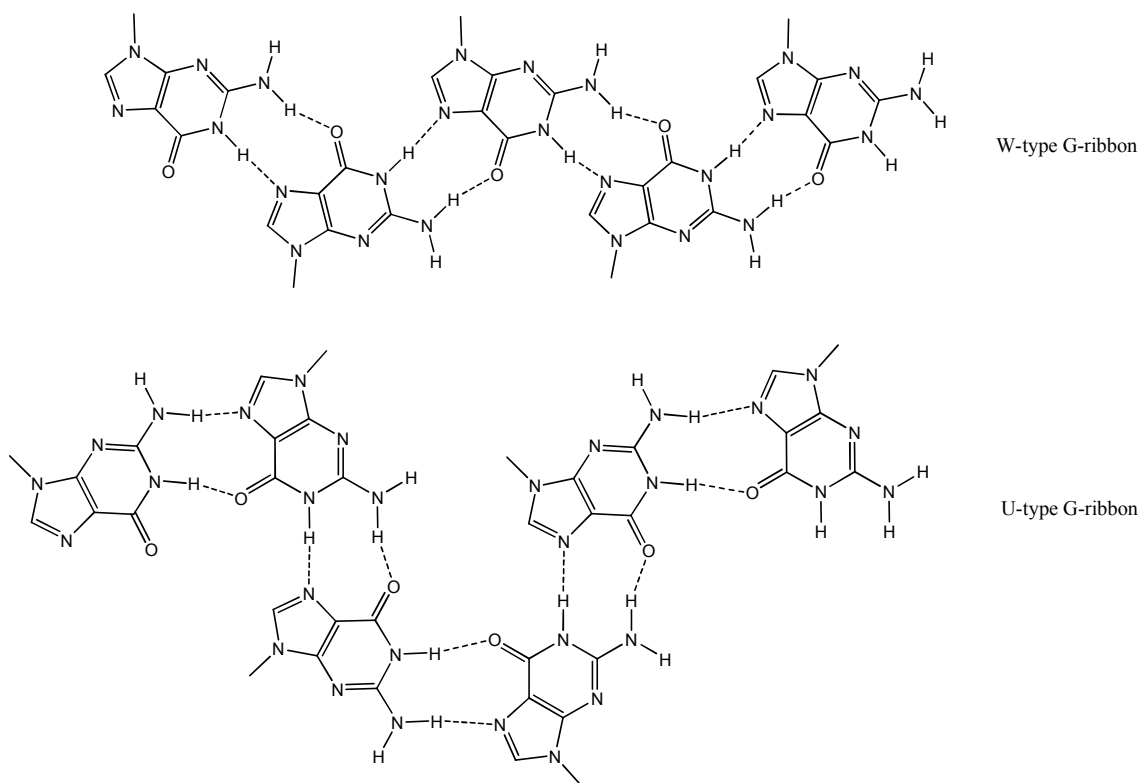


Figure S8. Schematic representation of the N^9 -methylguanine in its W and U ribbon assembly.

3. X-ray powder patterns N^3 -methylxanthine (compound 1)

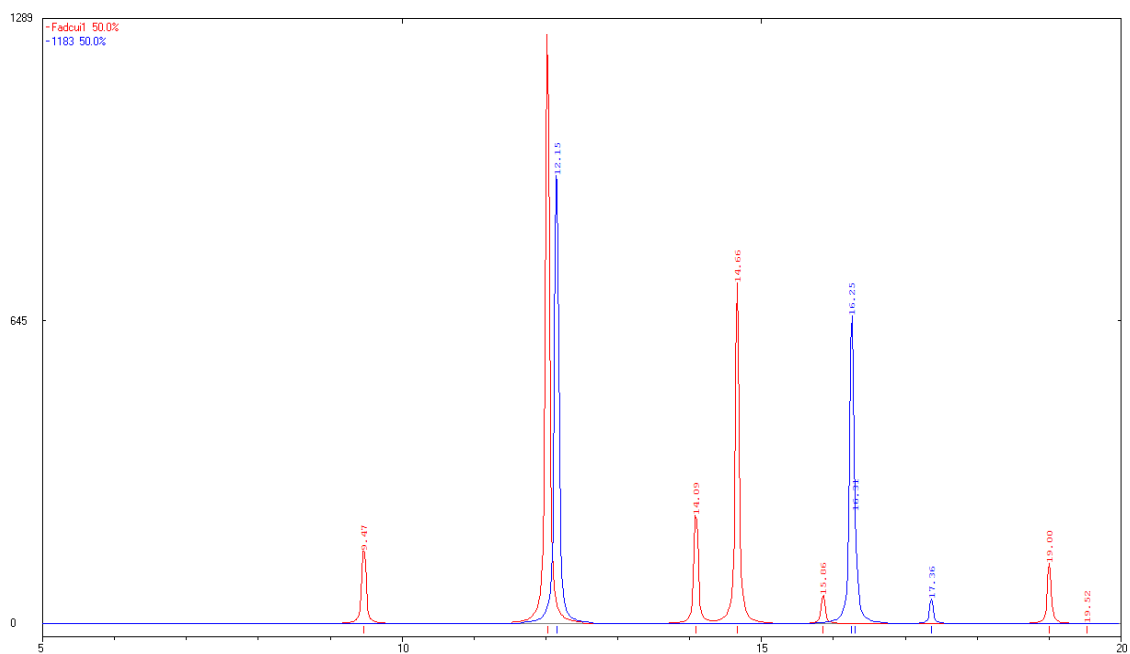


Figure S9. The calculated X-ray powder pattern for the literature (red) and the new polymorphic structure (blue) of N^3 -methylxanthine (compound 1).¹

4. X-ray crystal structures of FADCUI and N^3 -methylxanthine (1)

Table S1. Crystallographic data and structure refinement results for N^3 -methylxanthine (1).

Name	N^3 -methylxanthine
Formula	$C_6H_6N_4O_2$
Formula weight	166.15
Crystal system	Orthorhombic
Space group	Pc2 ₁ b (No. 29)
$a / \text{\AA}$	5.449(5)
$b / \text{\AA}$	8.160(5)
$c / \text{\AA}$	14.558(5)
$V / \text{\AA}^3$	647.3(7)
Z	4
$D_c / \text{g cm}^{-3}$	1.705
$F(000)$	344
μ / mm^{-1}	0.13
Reflections collected	1125
Unique reflections with $I > 2\sigma(I)$,	785
Parameters refined	116
GOF on F^2	1.17
$R[F^2 > 2\sigma(F^2)]$	0.097
$wR(F^2)$	0.238
$\Delta\rho_{\text{max}}, \Delta\rho_{\text{min}} / \text{e \AA}^{-3}$	0.35, -0.37

Table S2. Bond length data for the new polymorph and the literature structure (FADCUI)¹ of *N*³-methylxanthine.

	New polymorph	FADCUI
C2 - O2	1.214(9)	1.218
C2 - N3	1.367(12)	1.364
C2 - N1	1.389(10)	1.389
C4 - C5	1.324(10)	1.370
C4 - N9	1.327(10)	1.341
C4 - N3	1.392(9)	1.381
C5 - N7	1.385(9)	1.372
C5 - C6	1.457(14)	1.397
C6 - O6	1.222(10)	1.225
C6 - N1	1.373(10)	1.382
C8 - N7	1.319(12)	1.323
C8 - N9	1.344(9)	1.326
C9 - N3	1.469(9)	1.468
N1 - H1	0.86(2)	0.891
N7 - H7	0.87(2)	0.838

Table S3. Hydrogen-bond geometry of the new polymorph of *N*³-methylxanthine (**1**).

<i>D</i> —H \cdots <i>A</i>	<i>D</i> —H (Å)	H \cdots <i>A</i> (Å)	<i>D</i> \cdots <i>A</i> (Å)	<i>D</i> —H \cdots <i>A</i> (°)
NH(1) \cdots N(9) ⁱ	0.86	2.18	3.010 (10)	163
NH(7) \cdots O(2) ⁱⁱ	0.87 (2)	1.97 (5)	2.774 (9)	154 (10)

Symmetry codes: (i) $x+1, y+1/2, -z+1/2$; (ii) $-x+2, y, z-1/2$.

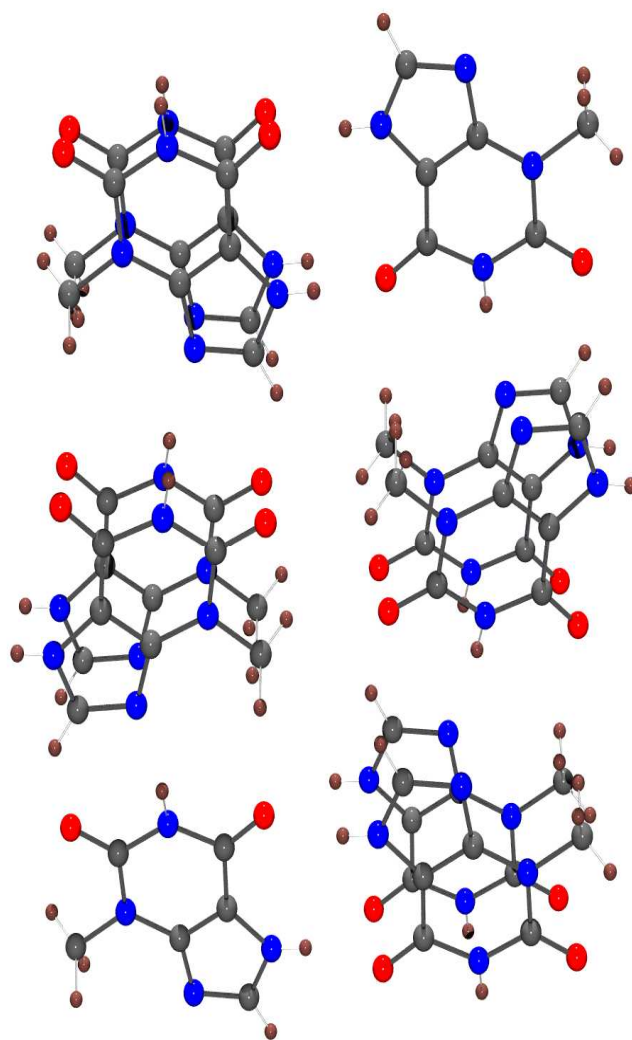


Figure S10. Stacking motif in FADCUI X-ray structure showing the parallel orientation of alternating rings. View normal to (100).

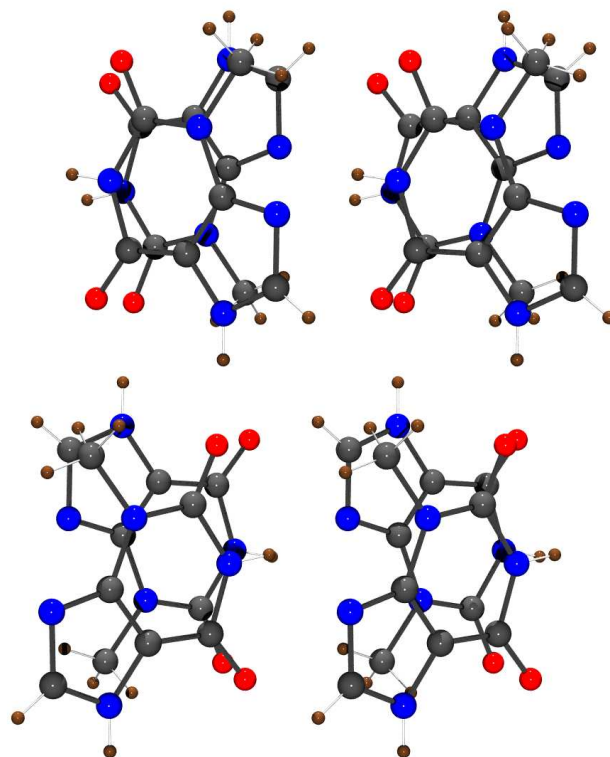


Figure S11. Stacking motif in new polymorph of **1** showing the rotated orientation of alternating rings. View normal to (010)

5. Theoretical studies

Table S4. Calculated (BLYP-D/TZ2P level of theory) total bonding energies and average H-bonding energies (in kcal/mol) of 4, 6, 8, 10 and 12 units long optimized X and G ribbons.

no. of units in ribbon	Total bonding energies (in kcal/mol)				Average stabilization energies (in kcal/mol) per H-bond.			
	X-W	X-U	G-W	G-U	X-W	X-U	G-W	G-U
4	-58.5	-57.7	-66.1	-64.8	-9.8	-9.6	-11	-10.8
6	-95.2	-95.2	-114.3	-116.5	-9.5	-9.5	-11.4	-11.7
8	-131.7	-128	-162.9	-165.3	-9.4	-9.1	-11.6	-11.8
10	-169.1	-169.6	-211.8	-213.7	-9.4	-9.4	-11.8	-11.9
12	-204.9	-205.3	-260.5	-262.5	-9.3	-9.3	-11.8	-11.9

X – N^3 -methylxanthine, G – N^9 -methylguanine, W and U – types of H-bonded ribbon.

References:

1. Low, J. N.; Tollin, P.; Brand, E.; Wilson, C. C., Structure of 3-Methylxanthine. *Acta Cryst. Sect. C* **1986**, 42, 1447-1448.